

# Evaluation of an automatic lean meat percentage quantification method based on a partial volume model from computed tomography scans

Pau Xiberta<sup>a,\*</sup>, Anton Bardera<sup>a</sup>, Imma Boada<sup>a</sup>, Marina Gispert<sup>b</sup>, Albert Brun<sup>b</sup>, Maria Font-i-Furnols<sup>b</sup>

<sup>a</sup>*Graphics and Imaging Laboratory, Universitat de Girona, 17003 Girona, Catalonia.*

<sup>b</sup>*IRTA-Food Industries, Finca Camps i Armet, E-17121 Monells, Girona, Catalonia.*

---

## Abstract

The quality of a pig carcass is mainly measured by the lean meat percentage (LMP), which can be virtually estimated from computed tomography (CT) scans. Different strategies exist to classify the CT voxels into tissues such as fat, lean and bone, being the thresholding-based methods the most commonly used. However, these methods are usually affected by the partial volume effect, and also by data variability, which is implicit from different CT scanners and protocols, since no standard behaviour has been defined. The aim of this paper is to extend an LMP quantification method which uses a partial volume model by adding a new step to detect the animal skin, and thoroughly evaluate the new approach by analysing each of its steps. The evaluation is performed by comparing the whole pipeline of the proposed approach with a simple thresholding method and a thresholding method with bone filling and skin detection, which is an intermediate step of the new

---

\*Corresponding author

*Email addresses:* `pau.xiberta@udg.edu` (Pau Xiberta), `anton.bardera@udg.edu` (Anton Bardera), `imma.boada@udg.edu` (Imma Boada)

pipeline. Five experiments have been designed to test how accurate are the results of the method regarding the LMP values computed from the manual dissection, as well as the robustness to data variability. Two different manual dissection methodologies have been tested: the partial dissection, which estimates the LMP using the lean of the four main cuts of the carcass plus the tenderloin, and the total dissection, which uses the lean of the twelve main cuts. A total of 146 half carcasses have been used for this study (105 using the partial dissection methodology, and 41 using the total dissection one). To evaluate the experiments, the LMP values virtually obtained from the three methods have been compared mostly with the LMP values from the manual dissection, computing the coefficient of determination  $R^2$  from the correlations, as well as the root mean square error of prediction by means of leave-one-out cross-validation. A statistical analysis is performed to resolve if two correlations are significantly different. The experiments' results confirm the high accuracy of the proposed approach for the LMP estimation, and mainly its high robustness to data variability. The experiments also disclose that the detection of the animal skin and its classification as a new tissue, instead of classifying it as lean, improve the results. The evaluated method has demonstrated to be as effective as the thresholding method with bone filling and skin detection, and more robust to data variability than the other evaluated methods.

*Keywords:* Lean meat percentage, Computed tomography, Partial volume effect, Segmentation, Pig carcass quantification

---

## 1. Introduction

Lean meat percentage (LMP) is a key parameter to measure pig carcass quality, it is compulsory in the Europe Union and it determines the basis for the price of the carcass. To compute the LMP from computed tomography (CT) scans, special methods to classify CT voxels into tissues according to its Hounsfield Unit (HU) values are required. Unfortunately, variability between animals and breeds, and also between scanners and protocols makes the definition of a standard correspondence between HU values and tissues difficult (Olsen et al. (2017)), and each country has defined its own model (Romvári et al. (2006); Font-i-Furnols et al. (2009); Daumas and Monziols (2011)). Moreover, the partial volume effect further complicates LMP computation, that is, voxels which are usually placed in the border between two tissue regions may have a big uncertainty, and they cannot be classified because they contain more than one tissue. This difficulty has been studied in other fields such as oncology (see Cysouw et al. (2017) for a review), but mainly in the field of neuroimaging (see Tohka (2014) for a review), evaluating its impact (Dukart and Bertolino (2014)), compiling different methods to enhance the image visualisation (Salminen et al. (2016)), and still proposing novel techniques to reduce the effect (Bural et al. (2015); Şener et al. (2016)).

To tackle the partial volume problem, different strategies have been proposed. Assuming a uniform probability for the non-pure tissues over the image, i.e. each partial volume voxel has the same probability for every non-pure tissue, Santiago and Gage (1993) propose a model with six Gaussian distributions, three for the pure tissues and three for the two-class partial volume ones, with a set of parameters which have to be minimised to fit the

26 model to the histogram. With the same assumption, Laidlaw et al. (1998)  
 27 reconstruct a continuous function incorporating neighbouring voxels informa-  
 28 tion into the classification process to improve its accuracy, and Ruan et al.  
 29 (2000) first use a mixture model to define a Gaussian distribution for each  
 30 pure and partial volume tissue, and then reclassify the partial volume classes  
 31 into the pure ones using a Markov random field and multifractal analysis.

32 Other studies assume little variation in the probability for the non-pure  
 33 tissues between neighbouring voxels, which can be modelled using a Markov  
 34 random field. Choi et al. (1991) use a maximum *a posteriori* estimation of  
 35 partial volume voxels in multichannel images, and a method to iteratively  
 36 reestimate the mean intensities of each tissue class in each slice, while Pham  
 37 and Prince (2000) propose a similar method for single-channel images using a  
 38 Bayesian approach which places a prior probability model on the parameters.  
 39 Finally, Nocera and Gee (1997) describe a segmentation algorithm which also  
 40 uses a maximum *a posteriori* estimation with an adaptive Bayesian approach,  
 41 and takes into account both the partial volume and the shading effect.

42 Focusing on the LMP computation, several methods have been presented  
 43 in the literature. Gangsei et al. (2016) and Jansons et al. (2016) use optical  
 44 probes to collect certain variables, which is an efficient method when work-  
 45 ing with carcasses, and in Dobrowolski et al. (2004), Judas et al. (2007) and  
 46 Font-i-Furnols et al. (2009) data from CT images is analysed using partial  
 47 least squared regression, which does not require the classification of voxels  
 48 in lean or fat. In this case, volume associated to each HU value is obtained  
 49 from CT images and used as predictors in the regression. To build their re-  
 50 gression equations, Kremer et al. (2013) and Bernau et al. (2015) use linear

51 traits measured by dual energy X-ray absorptiometry (DXA), while Lisiak  
 52 et al. (2015) proposes a simpler approach using linear measurements over  
 53 the carcass which do not need the use of expensive classification equipment.  
 54 Another common method is to use thresholding techniques based on the HU  
 55 values (Daumas and Monziols (2011)), and even mixing thresholding tech-  
 56 niques with some manual interaction in a semi-automatic method (Bernau  
 57 et al. (2015)). Kongsro et al. (2008) have applied a thresholding approach us-  
 58 ing lamb meat as well, and Lee et al. (2015) have adopted a similar method  
 59 using beef, the latter also using a chemical analysis to compare the results  
 60 with the thresholding method. To avoid dealing with the partial volume  
 61 effect when using the thresholding techniques, some strategies have been  
 62 proposed. In Vester-Christensen et al. (2009) the partial volume effect has  
 63 been minimised applying a Bayesian 2D contextual classification scheme to  
 64 classify voxels into fat, lean and bone. Differently, in Bardera et al. (2014)  
 65 a five-step process which automatically quantifies fat, lean, and bone tissues  
 66 from CT scans using a partial volume model based on the one presented by  
 67 Van Leemput et al. (2003) is described, and a first validation of the method  
 68 considering 10 carcasses is carried out.

69 The aim of this paper is to evaluate the quantification method presented  
 70 in Bardera et al. (2014) considering 146 half carcasses which have been man-  
 71 ually dissected after scanning (105 using a partial dissection, and 41 using  
 72 a total dissection). The introduction to the method’s pipeline of a new step  
 73 which identifies and classifies the animal skin tissue is also analysed. The  
 74 obtained results are compared in terms of LMP accuracy and robustness  
 75 to data variability, and the importance and need for each step of the new

76 pipeline is discussed.

## 77 **2. Materials and methods**

### 78 *2.1. Carcasses and computed tomography scanning*

79 A total of 146 left half carcasses have been used for this study. From these,  
80 133 carcasses come from two commercial abattoirs and have been selected to  
81 mimic the Spanish pig carcass population in terms of fat thickness, being all  
82 the three sexual types represented. These carcasses also come from several  
83 producers and commercial genotypes. Additionally, 13 carcasses from gilts,  
84 slaughtered at the pilot abattoir placed at IRTA-Monells, have also been used  
85 in this study. These carcasses are from 3 different genotypes as described in  
86 Carabús et al. (2014) and Font-i-Furnols et al. (2015). In total, carcasses  
87 included in this study have a carcass weight of  $86.7 \pm 8.7$  kg, a fat thickness  
88 of  $15.7 \pm 3.8$  mm measured at 6 cm of the midline between the 3rd and the  
89 4th last ribs, and they are from three sexual types (47% females, 41% entire  
90 males and 12% castrated males). The Commission Delegated Regulation  
91 (EU) 2017/1182 (The European Commission (2017)) established a minimum  
92 of 120 carcasses representative of the population to be involved in a dissection  
93 trial. For this reason, the number and type of carcasses considered in this  
94 work is suitable to be used to evaluate the methodology proposed in this  
95 paper to determine carcass lean meat content.

96 At 24-48 h post mortem carcasses were CT scanned with a General Elec-  
97 tric HiSpeed Zx/I device placed at IRTA-Monells. Acquisition parameters  
98 were those established by Font-i-Furnols et al. (2009) in carcasses evaluation,  
99 that is, 140 kV, 145 mA, Display Field of View (DFOV) between 460 and 500

100 mm, and matrix size 512×512 pixels. Images were acquired helically every  
101 10 mm with pitch 1. Thus, there was not overlapping between images and  
102 all the carcasses were scanned completely.

### 103 *2.2. Manual dissection*

104 After scanning, carcasses were cut following the Walstra and Merkus  
105 method (Walstra and Merkus (1996)) and dissected by trained butchers.  
106 A total of 105 carcasses were dissected using the partial dissection method-  
107 ology, i.e. the lean from the four main cuts (ham, shoulder, belly and loin)  
108 was manually separated with a knife and weighed. The LMP values were  
109 obtained dividing the weight of the lean of the four main cuts plus the ten-  
110 derloin by the total weight of the four main cuts plus the tenderloin. A  
111 correction factor of 0.89 was applied to obtain the LMP values of the car-  
112 casses from these cuts, according to the European Regulation definition (The  
113 Commission of the European Communities (2008)). The other 41 carcasses  
114 were totally dissected, i.e. the lean of all the 12 cuts was manually obtained  
115 and weighed, and this weight was divided by the weight of the carcass to  
116 obtain the LMP (The Commission of the European Communities (2008)).

### 117 *2.3. Automatic LMP quantification method based on a partial volume model*

118 The proposed approach to quantify fat, lean and bone from CT carcasses  
119 is an improvement of the method presented in Bardera et al. (2014). We  
120 propose to extend this automatic five-step method with a new step which  
121 detects the animal skin. The six steps are illustrated in Figure 1 and de-  
122 scribed below. For more details see Bardera et al. (2014).

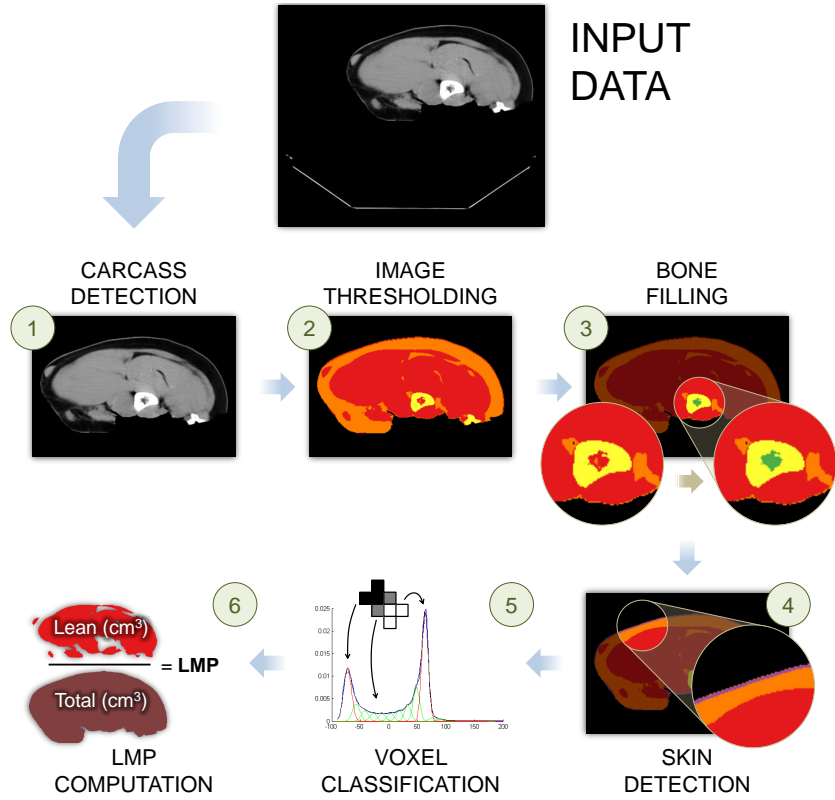


Figure 1: The six main steps of the proposed approach to compute the LMP values from pig carcasses CT images.

123     **1. Carcass detection.** The pig carcass is detected from the input CT  
 124     scans, and other structures of the image such as the scanning table and  
 125     the air are removed. Taking into account that the carcass lies over a  
 126     cushion which has intensity values similar to those of the air, cropping  
 127     the bottom part of the image is enough to remove the table and other  
 128     supporting elements. Then, the carcass is only surrounded by voxels  
 129     with very low intensities (air and cushion), and it can be detected using  
 130     a simple thresholding method.



- 131     **2. Image thresholding.** A thresholding technique based on the HU val-  
132     ues is applied in order to pre-identify fat, lean and bone tissues. By  
133     default, a value of -100 HU has been defined as a threshold between  
134     air/background and fat, 0 HU between fat and lean, and 120 HU be-  
135     tween lean and bone (Font-i-Furnols et al. (2009)).
- 136     **3. Bone filling.** Since the marrow tissue is often confused with fat in the  
137     thresholding step, the marrow surrounded by bone tissue is also con-  
138     sidered as bone. To achieve this result, a binary hole filling operation  
139     is carried out from the 2D bone mask obtained in the previous step.
- 140     **4. Skin detection.** Although it represents a little part of the whole  
141     carcass, the skin tissue should not be confused with the lean tissue,  
142     as both tissues have similar HU values. Knowing that the skin is the  
143     outermost tissue, and that the subcutaneous fat separates it from the  
144     lean tissue, a measure to detect the skin voxels is proposed, avoiding by  
145     this way to take them into account when computing the LMP values.  
146     All the voxels with values lying in the HU range of lean tissue are  
147     filtered so that the ones at 3 mm from the background are considered  
148     as skin. The distance is computed using a background binary mask  
149     obtained from the carcass detection in the first step, and a distance  
150     filter which measures the Euclidean distance of each voxel of the mask  
151     to the background. Once the distance is computed, a filtering process is  
152     applied in order to keep only those lean voxels obtained in the second  
153     step whose distance to the background is 3 mm or less, taking into  
154     account the size of a voxel, which in this case approaches 1 mm<sup>3</sup>. This is  
155     the new step introduced in the method with respect to the one proposed

by Bardera et al. (2014).

**5. Pure class identification and partial volume model.** The pure and partial volume voxels are classified using the partial volume model without spatial correlation proposed by Van Leemput et al. (2003), which includes an iterative expectation-maximisation algorithm. In this case, the input of the method is just the histogram, leading to a very fast process, and the output is the probability of each intensity value to belong to the fat, lean or bone tissues. To compute the amount of voxels for the lean tissue, for example, all the voxels' probabilities of belonging to the lean tissue are added up, resulting in the estimated total number of lean voxels. Thus, a single voxel can contribute to the sum of different tissues. Figure 2 shows an original CT image and the partial volume classification of its voxels, including a separate image for each tissue indicating the probability of each voxel of belonging to it. Note the partial volume effect between the background and the already removed skin tissue in the carcass border of the fat voxels classification image.

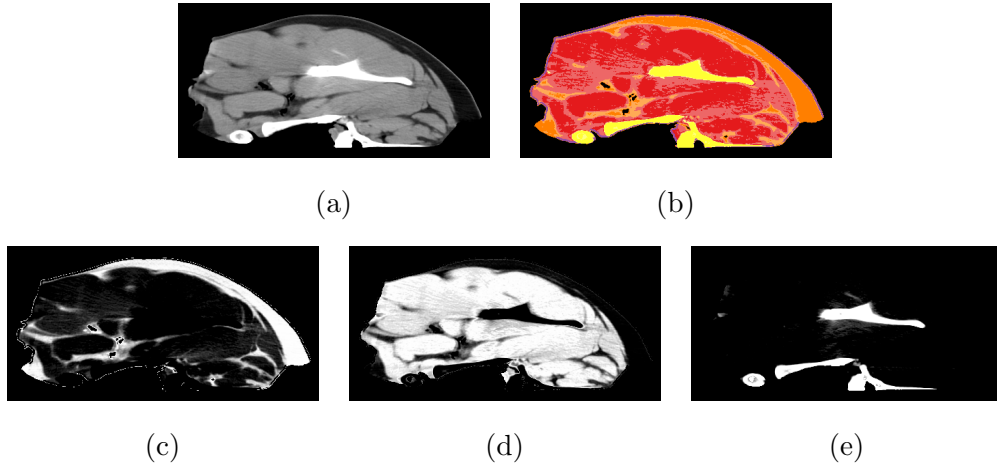


Figure 2: Partial volume classification of a particular CT image: (a) original CT image; (b) pure tissues (probability  $> 90\%$ , strong colours) and partial volume voxels ( $50\% < \text{probability} < 90\%$ , pale colours), where orange = fat, red = lean, yellow = bone, and purple = skin (skin is not considered in the partial volume classification); (c, d, e) probability of each voxel of belonging to the fat, lean and bone tissues, respectively (white = 100% probability, black = 0% probability).

173     **6. LMP computation.** The volume of the lean meat obtained from  
 174     the partial volume classification is divided by the volume of the whole  
 175     carcass, including all the tissues. The result is the lean meat percentage,  
 176     that is, the value of interest. To compute the volume, the corresponding  
 177     number of voxels is multiplied by the volume of a single voxel.

#### 178     2.4. Software implementation

179     The proposed approach has been implemented using C++, Qt, the Insight  
 180     Toolkit (ITK) and the Visualisation Toolkit (VTK) libraries as a new module  
 181     of the VisualPork software (Bardera et al. (2012)). VisualPork is an in-house  
 182     software which supports DICOM standard and IHE profiles, integrates image

183 processing techniques, and provides 2D and 3D visualisation functionalities.  
184 It has been developed at the Graphics and Imaging Laboratory (GILAB)  
185 from the University of Girona in collaboration with experts from IRTA-Food  
186 Industries.

## 187 2.5. *Evaluation metrics*

188 The goal of the proposed approach is to find a method which is able to  
189 compute the LMP values from a pig carcass, with the purpose of getting a  
190 value as close as possible to the manually computed LMP. Thus, the first  
191 measure to be taken into account when analysing the CT images from the  
192 carcasses is the LMP, which is the ratio of the lean meat voxels to the total.

193 To compare the virtually obtained LMP values with the manually ob-  
194 tained ones, a correlation between these values is needed. Indeed, this cor-  
195 relation is needed to compare between two different methods, and also to  
196 compare between different ways of using the same method. The coefficient  
197 of determination  $R^2$  (i.e. the square of the correlation coefficient  $R$ ) will be  
198 used to analyse the correlations.

199 Considering the LMP values obtained from the manual dissection as the  
200 true value, the root mean square error of prediction (RMSEP) can also be  
201 computed by means of leave-one-out cross-validation as another measure of  
202 accuracy.

203 Finally, to determine whether the differences between the correlations of  
204 two different methods are significant, several statistical tests for comparing  
205 two correlations based on dependent groups with overlapping variables can  
206 be applied, being one of the most representative the one proposed by Steiger  
207 (1980). To apply these tests, the tool implemented by Diedenhofen and

208 Musch (2015) will be used with a significance level of 0.05.

## 209 2.6. Experiments' description

210 To evaluate the proposed approach and other related methods, different  
211 experiments have been carried out to determine whether the proposed ap-  
212 proach can be selected as a method of reference to compute the LMP values  
213 of pig carcasses. Each experiment proposes alternatives of the pipeline de-  
214 scribed in Figure 1, and they are compared at least to the manual dissection  
215 results. Figure 3 shows a diagram where the alternatives of the pipeline are  
216 represented, always taking into account the 6 steps from the original pipeline.  
217 The experiments have been designed to evaluate the importance of each one  
218 of these steps. As previously mentioned, two different methodologies have  
219 been used to perform the manual dissection: the partial dissection, and the  
220 total dissection. All the experiments have been executed separately, using a  
221 different set of carcasses for each situation.

222 *Experiment 1.* In the first experiment, three methods to compute the  
223 LMP values have been compared to the manual dissection, which is consid-  
224 ered as the reference model. These methods include a simple thresholding  
225 segmentation (Gonzalez and Woods (2002)), a thresholding with bone filling  
226 and skin detection, and the proposed partial volume approach. The first  
227 one can be considered as the base method, since only a simple thresholding  
228 segmentation is performed (first to second step of the pipeline represented in  
229 Figure 1, plus the sixth step to compute the LMP value). The second one is  
230 an extension of the base method, applying also a bone filling operation and  
231 the new skin detection step described in Section 2.2 (first to fourth step of  
232 the pipeline, plus the sixth step). Finally, the last method corresponds to

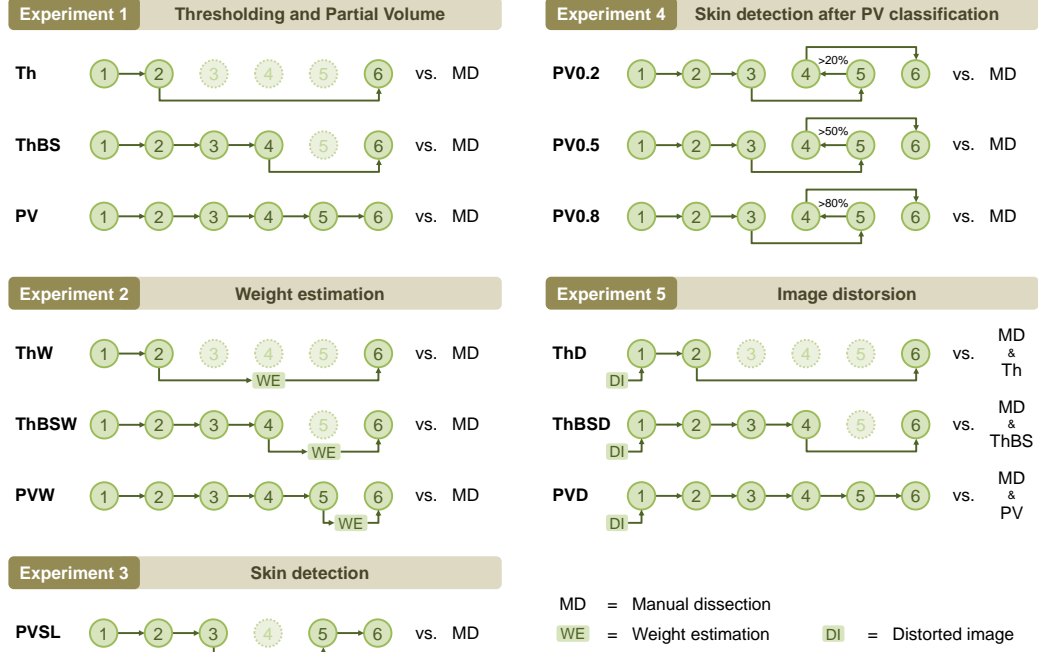


Figure 3: Steps from the whole pipeline which are part of the different alternatives analysed in each experiment.

the whole proposed approach, including the application of a partial volume model. The correlations of the different strategies have been computed to know which method better approximates the LMP values.

*Experiment 2.* While the CT scans of pig carcasses provide a good means to obtain the volume of each tissue by counting the number of voxels, the LMP values of the manual dissection are based on weights. To simulate this procedure, a density estimation is needed to compute the weight of the segmented tissues once the number of voxels of each one is known. However, the second experiment aims to show that the results of the algorithm are not improved when the density estimation is applied and the voxels are assigned

different weights, i.e. when the results take into account the weight, not the volume. As for the pipeline of this testing method, a new step corresponding to the weight estimation is included before the sixth step, which refers to the LMP computation. The model proposed by Vester-Christensen et al. (2009) has been followed to estimate the tissues' weights. The correlation between the weight-based results and the manual dissection has been computed, so that it can be compared with the results of the previous experiment.

*Experiment 3.* When using thresholds to segment the tissues from a carcass, the segmentation of the skin is troublesome, since the skin voxels have values very similar to the lean voxels' values. To solve this problem, all the voxels considered as lean which are at a distance of 3 mm from the background are considered as skin (see the fourth step of Figure 1). Thus, these voxels are not computed as lean when obtaining the LMP values, i.e. the skin tissue is not taken into account in the numerator of the LMP computation. The third experiment compares the results considering the skin as lean, i.e. ignoring the fourth step of the pipeline, with the results considering the skin as a new tissue. The correlation between the results considering the skin as lean and the manual dissection has been computed, so that it can be compared with the results of the first experiment, which considers the skin as a new tissue.

*Experiment 4.* The detection of the skin is based on thresholding methods, and it is performed before the partial volume classification. However, a voxel may be composed of skin and fat tissues at the same time (see Figure 2c), so the partial volume classification could be applied before the skin detection step. This is exactly the purpose of the fourth experiment, which swaps the

268 fourth and the fifth step of the pipeline. Since the partial volume classifi-  
 269 cation outputs a tissue probability for each voxel, the probability threshold  
 270 has to be defined in order to determine when a skin voxel can be considered  
 271 as so. Assuming that the intensity values of skin voxels are similar to those  
 272 of lean voxels, the lean tissue probability is taken into account. Hence, a  
 273 voxel is considered to belong to the skin tissue when it is at 3 mm from the  
 274 background and its probability to belong to the lean tissue is more than the  
 275 defined threshold. Three different thresholds have been selected: 0.2 (20%  
 276 probability of belonging to the lean tissue), since it is the value which obtains  
 277 the best results; 0.5 (50% probability), since it is the more reasonable value  
 278 to discern between fat and lean tissues; and 0.8 (80% probability), to include  
 279 a more restrictive value. The correlation between the results swapping the  
 280 fourth and fifth steps and the manual dissection has been computed, so that  
 281 it can be compared with the results of the first experiment, which performs  
 282 the skin detection step before the partial volume classification.

283 *Experiment 5.* Measurements of the same carcass using CT scanners from  
 284 different vendors may show variation because of several factors, including  
 285 the convolution kernel, reconstruction artefacts, beam hardening, spectral  
 286 energy, and scatter, as well as variations in carcass size, shape, and position  
 287 in scanner (Lamba et al. (2014); Mackin et al. (2015)). Moreover, although  
 288 the difference is not so significant, measurements using the same scanner can  
 289 also show variation (Jacobsen et al. (2016); Symons et al. (2016)). For this  
 290 reason, the last experiment modifies the original CT images to simulate this  
 291 image variability. Similarly to Bardera et al. (2014), a distortion function  
 292 given by  $HU_{scale} \times value + HU_{shift}$  has been applied to the values of all CT



scan voxels, where  $HU_{scale}$  takes a value randomly generated between 0.97 and 1.03, and  $HU_{shift}$  takes a value between -20 and 20. Note that this distortion is different for each carcass, but the same for all voxels of the same carcass, so that noise is not added to the image, but only a global transform that will modify the histogram with a scaling factor and a shift. To find out which method best tolerates data variation, the correlation between each method with distortion and the manual dissection has been computed, as well as the correlation between the distorted results and the ones without distortion.

### 3. Results and discussion

In this section, the results of the experiments described in Section 2.5 are presented and discussed, always discerning between the partial dissection and the total dissection methodologies. The experiments aim to show how the proposed approach improves the LMP computation.

The results of the first experiment for the partial dissection methodology are shown in Figure 4, where the scatter plot between each method and the manual dissection is represented, and the  $R^2$  and RMSEP values are given. The proposed approach (that is, the partial volume method) and the thresholding with bone filling and skin detection, which is an intermediate step of the proposed pipeline, clearly get the best results, with no significant differences between them (see Table 1 for the p-values). Similarly, the results for the total dissection methodology are shown in Figure 5, where there are no significant differences between the proposed approach and the thresholding with bone filling and skin detection either. However, although it has the lowest one, in this case the simple thresholding method also achieves a high

317 correlation, with nearly significant differences with respect to the proposed  
 318 approach. As for the computational time, although the code has not been  
 319 optimised, the bone filling and skin detection steps take most of the time of  
 320 the two last compared methods. On the other hand, the simple thresholding  
 321 and the partial volume classification need almost no time, so that the most  
 322 efficient method is the simple thresholding (approximately 300 milliseconds),  
 323 followed by the thresholding with bone filling and skin detection and the  
 324 proposed approach, which take almost 5 seconds.

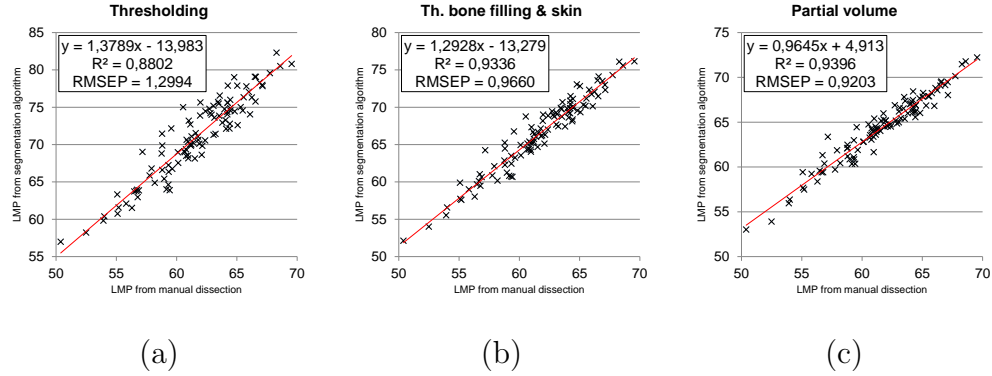


Figure 4: Correlation and error between each method and the manual dissection (partial dissection methodology).

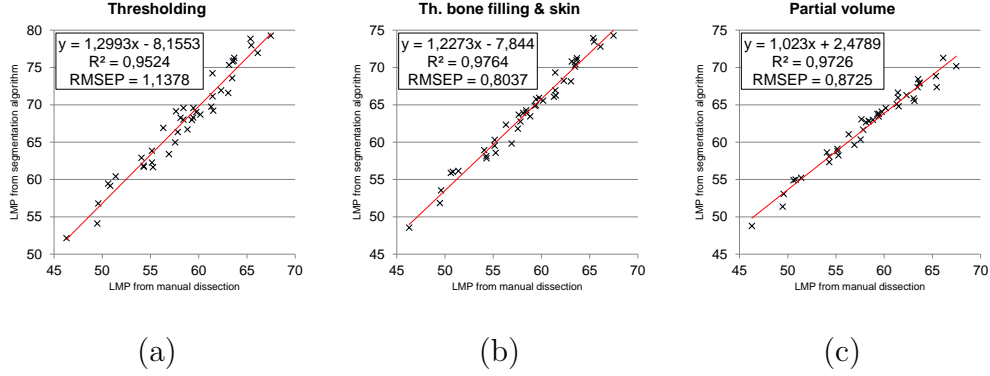


Figure 5: Correlation and error between each method and the manual dissection (total dissection methodology).

Dissection methodology	Compared correlations	min	max	Steiger
Partial	PV vs. Th	< 0.0001	0.0008	< 0.0001
	PV vs. ThBS	0.5161	0.5204	0.5195
Total	PV vs. Th	0.0597	0.0903	0.0616
	PV vs. ThBS	0.5978	0.6096	0.6072

Table 1: P-values of the comparison between the methods' correlations for the partial and the total dissection methodologies, showing the minimum and the maximum p-value from all the tests applied, and also the p-value of the Steiger's test (PV = Partial volume, Th = Thresholding, ThBS = Thresholding with bone filling and skin detection).

Regarding the second experiment, Figure 6 shows, for the partial dissection methodology and for each method, the scatter plot between the weight-based results (i.e. with density estimation) and the manual dissection, and also the  $R^2$  and RMSEP values. Similarly, Figure 7 shows it for the total dissection methodology. For the thresholding-based methods, and interpreting

330 the results for both dissection methodologies, the correlation and the error  
331 lead to believe that the best option is to estimate the density, while for the  
332 proposed approach they suggest that the best option is to take into account  
333 only the volume, not the weight. However, and for the proposed approach,  
334 there are not significant differences for the total dissection methodology, and  
335 only some tests state that there are significant differences for the partial  
336 dissection methodology (see Table 2 for the p-values). Since the density esti-  
337 mation has not been able to obtain a better result for the proposed approach,  
338 it will not be added as a new step of the pipeline.

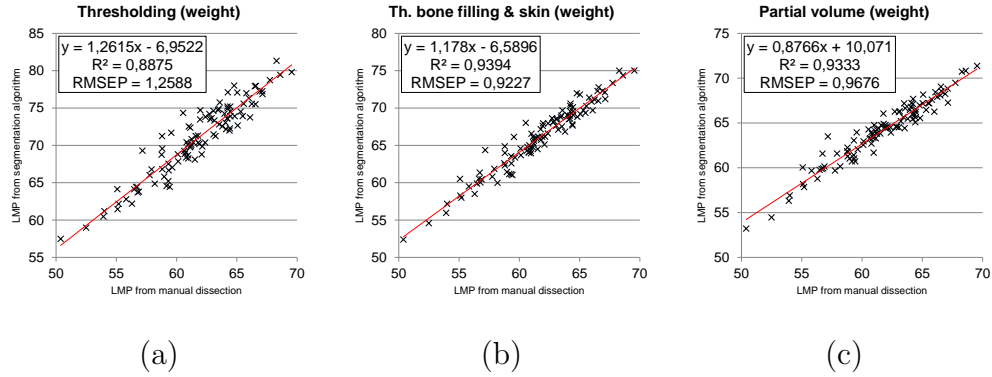


Figure 6: Correlation and error between each weight-based method and the manual dissection (partial dissection methodology).

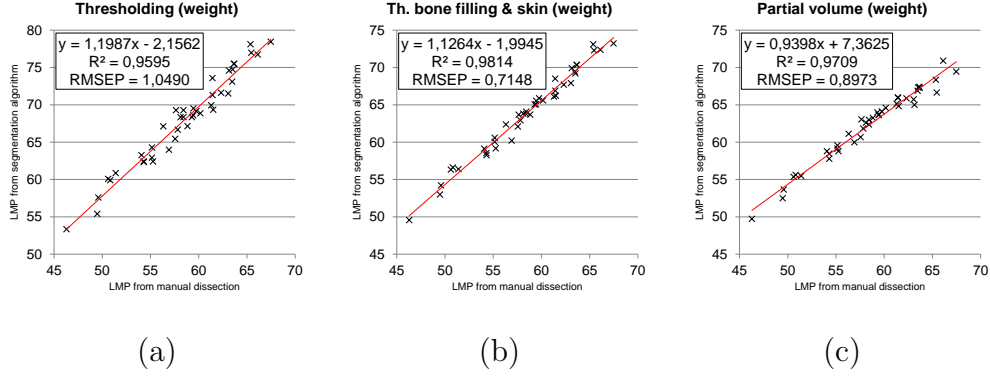


Figure 7: Correlation and error between each weight-based method and the manual dissection (total dissection methodology).

Dissection methodology	Compared correlations	min	max	Steiger
Partial	PVW vs. PV	0.0463	0.0589	0.0501
Total	PVW vs. PV	0.4930	0.5036	0.5019

Table 2: P-values of the comparison between the weight-based or volume-based correlations of the proposed approach for the partial and the total dissection methodologies, showing the minimum and the maximum p-value from all the tests applied, and also the p-value of the Steiger’s test (PV = Partial volume based on volume, PVW = Partial volume based on weight).

339 The third experiment analyses the importance of classifying the skin as  
340 a new tissue in the fourth step of the proposed pipeline. For both dissection  
341 methodologies, Figure 8 shows the scatter plot between the results consid-  
342 ering the skin as lean, i.e. ignoring the fourth step of the pipeline, and the  
343 manual dissection for the proposed approach, and also the  $R^2$  and RMSEP  
344 values ( $R^2 = 0.9016$  and  $RMSEP = 1.1764$  for the partial dissection, and  $R^2$

345 = 0.9467 and RMSEP = 1.2081 for the total dissection). The results con-  
 346 sidering the skin as a new tissue, and hence not considering it as lean when  
 347 computing the LMP values, i.e. considering all the steps of the pipeline, are  
 348 represented in Figure 4c and Figure 5c for the partial ( $R^2 = 0.9396$  and RM-  
 349 SEP = 0.9203) and the total ( $R^2 = 0.9726$  and RMSEP = 0.8725) dissection  
 350 methodologies, respectively. Clearly, the latter are much better and have sig-  
 351 nificant differences with respect to the former (see Table 3 for the p-values).  
 352 Two reasons can explain this outcome. Firstly, the manual dissection takes  
 353 into account the skin, so that it makes sense that detecting the skin in the  
 354 segmentation step helps to improve the results. Secondly, some voxels which  
 355 are close to the background may have a big uncertainty since it is difficult to  
 356 know the tissue where they belong; when assigning some of these voxels to  
 357 the skin tissue, the chances of assigning them to a wrong tissue disappear.  
 358 Therefore, skin detection can be considered as a necessary step.

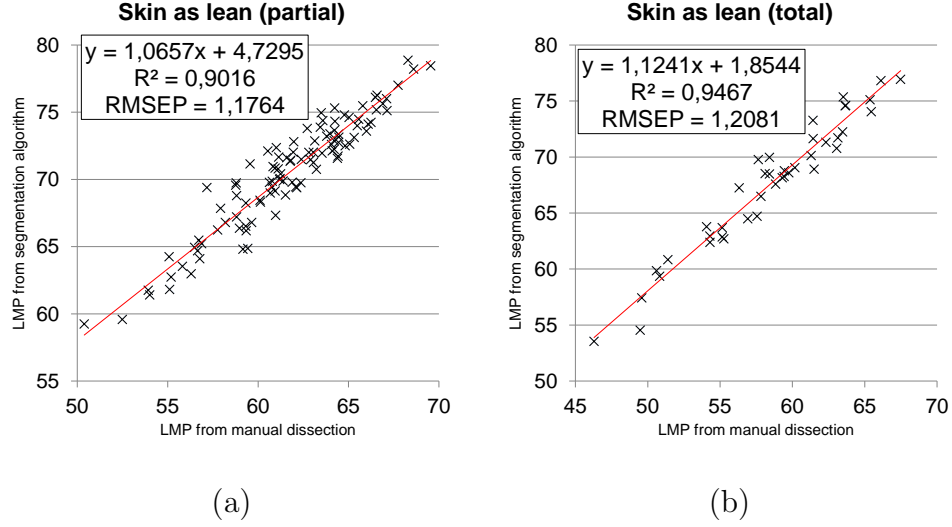


Figure 8: Correlation and error between the results of the proposed approach considering the skin as lean and the manual dissection (partial and total dissection methodologies).

Dissection methodology	Compared correlations	min	max	Steiger
Partial	PVSL vs. PV	< 0.0001	0.0009	0.0001
Total	PVSL vs. PV	0.0004	0.0141	0.0013

Table 3: P-values of the comparison between the proposed approach correlations considering the skin as lean (ignoring the skin detection step) or as a new tissue (considering all the steps) for the partial and the total dissection methodologies, showing the minimum and the maximum p-value from all the tests applied, and also the p-value of the Steiger’s test (PV = Partial volume considering the skin as a new tissue, PVSL = Partial volume considering the skin as lean).

359 The fourth experiment evaluates the results when applying the skin de-  
360 tection step after the partial volume classification, i.e. swapping the fourth  
361 and the fifth step of the pipeline. In this way, every voxel has a certain prob-

362 ability of belonging to each tissue, so that a probability threshold is needed  
 363 to determine if a voxel belongs to the skin tissue or not. Figure 9 shows,  
 364 for the partial dissection methodology and for the proposed approach, the  
 365 scatter plot between the results from the swapped pipeline and the manual  
 366 dissection for each tested threshold, and also the  $R^2$  and RMSEP values. Al-  
 367 though the correlation is higher when using the original pipeline ( $R^2 = 0.9396$   
 368 and  $\text{RMSEP} = 0.9203$ ), only when the probability threshold is established to  
 369 0.8 ( $R^2 = 0.9248$  and  $\text{RMSEP} = 1.0266$ ) the differences are significant (see  
 370 Table 4 for the p-values). Similarly, Figure 10 shows the same comparison  
 371 for the total dissection methodology. In this case, the results obtained using  
 372 the original pipeline ( $R^2 = 0.9726$  and  $\text{RMSEP} = 0.8725$ ) are significantly  
 373 better than the ones using the swapped pipeline, regardless of the probab-  
 374 ity threshold used (0.2 threshold:  $R^2 = 0.9690$  and  $\text{RMSEP} = 0.9256$ ; 0.5  
 375 threshold:  $R^2 = 0.9668$  and  $\text{RMSEP} = 0.9570$ ; 0.8 threshold:  $R^2 = 0.9570$   
 376 and  $\text{RMSEP} = 1.0863$ ). Overall, placing the skin detection after the partial  
 377 volume classification does not improve the results, and in some situations the  
 378 results are worse. Hence, the original pipeline is preferred.



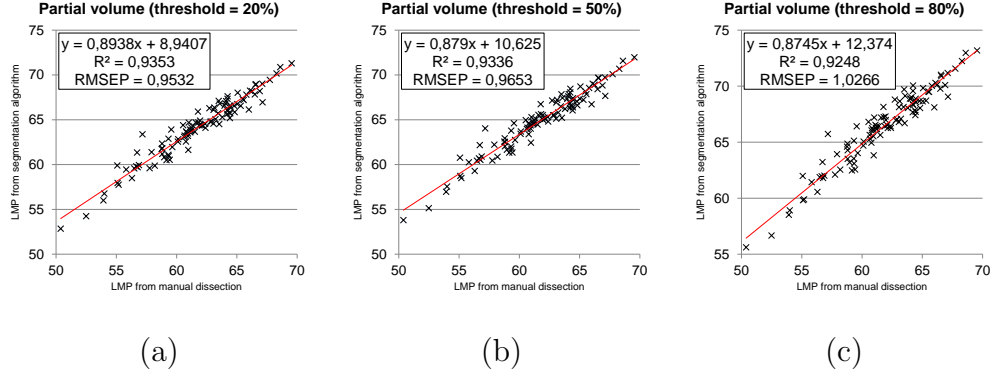


Figure 9: Correlation and error between the results of the proposed approach using the swapped pipeline (i.e. applying the skin detection step after the partial volume classification) and the manual dissection, taking into account three different probability thresholds, namely 0.2, 0.5 and 0.8 (partial dissection methodology).

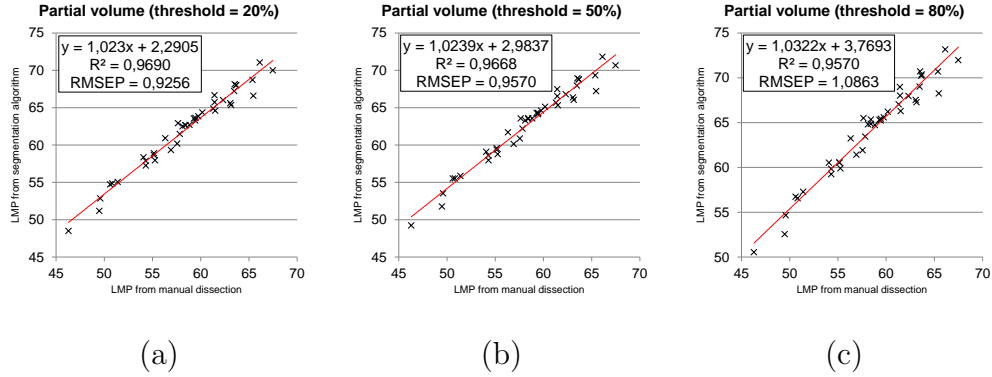


Figure 10: Correlation and error between the results of the proposed approach using the swapped pipeline (i.e. applying the skin detection step after the partial volume classification) and the manual dissection, taking into account three different probability thresholds, namely 0.2, 0.5 and 0.8 (total dissection methodology).

Dissection methodology	Compared correlations	min	max	Steiger
Partial	PV0.2 vs. PV	0.1925	0.1995	0.1957
	PV0.5 vs. PV	0.1130	0.1238	0.1167
	PV0.8 vs. PV	< 0.0001	0.0011	0.0001
Total	PV0.2 vs. PV	0.0029	0.0249	0.0070
	PV0.5 vs. PV	< 0.0001	0.0093	0.0005
	PV0.8 vs. PV	< 0.0001	0.0040	< 0.0001

Table 4: P-values of the comparison between the correlations of the proposed approach using the original pipeline or the swapped one (i.e. swapping the fourth and the fifth step of the pipeline) with three probability thresholds, namely 0.2, 0.5 and 0.8, for the partial and the total dissection methodologies, showing the minimum and the maximum p-value from all the tests applied, and also the p-value of the Steiger’s test (PV = Partial volume; PV0.2, PV0.5 and PV0.8 = Partial volume with swapped pipeline and probability threshold established to 0.2, 0.5 and 0.8, respectively).

379 Taking into account the results from the first experiment, the proposed  
380 approach achieves results similar to the ones obtained using an intermediate  
381 step, i.e. the thresholding segmentation with bone filling and skin detection.  
382 However, one of the main goals of the proposed approach, which is analysed  
383 in the last experiment, is to be robust on data variability. Figure 11 shows the  
384 results for the partial dissection methodology, where the scatter plot between  
385 each method with distortion and the manual dissection is represented, and  
386 the  $R^2$  and RMSEP values are given. Likewise, Figure 12 shows the results  
387 for the total dissection methodology. Furthermore, Figure 13 shows, for  
388 each method, the scatter plot between the distorted results and the ones  
389 without distortion, giving also the  $R^2$  and RMSEP values. In this case,

all the carcasses are taken into account, since the values compared in the correlations are all obtained from the virtual methods, and no differentiation between manual dissection methodologies is needed. The results show that the proposed approach (the whole proposed pipeline) is the most robust method to image variability, obtaining correlation ratios significantly higher than the thresholding-based methods (see Table 5 for the p-values).

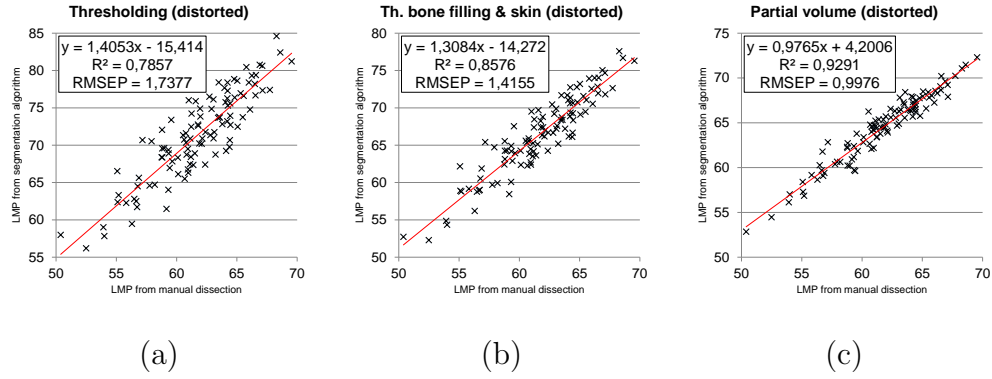


Figure 11: Correlation between each method with distortion and the manual dissection (partial dissection methodology).

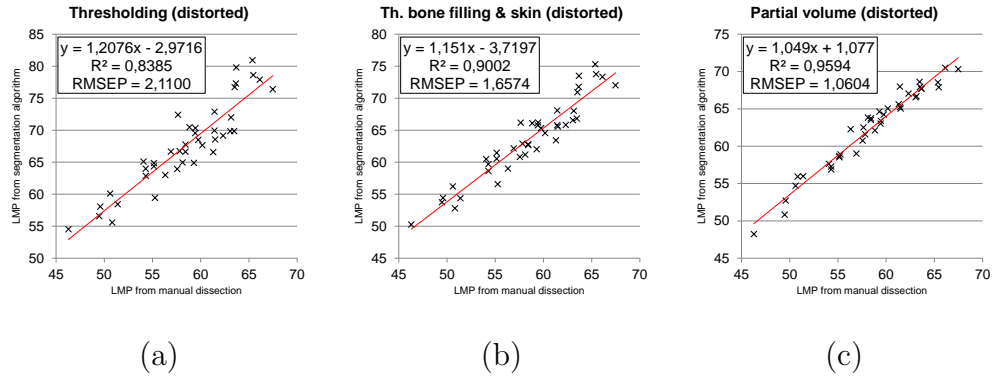


Figure 12: Correlation between each method with distortion and the manual dissection (total dissection methodology).

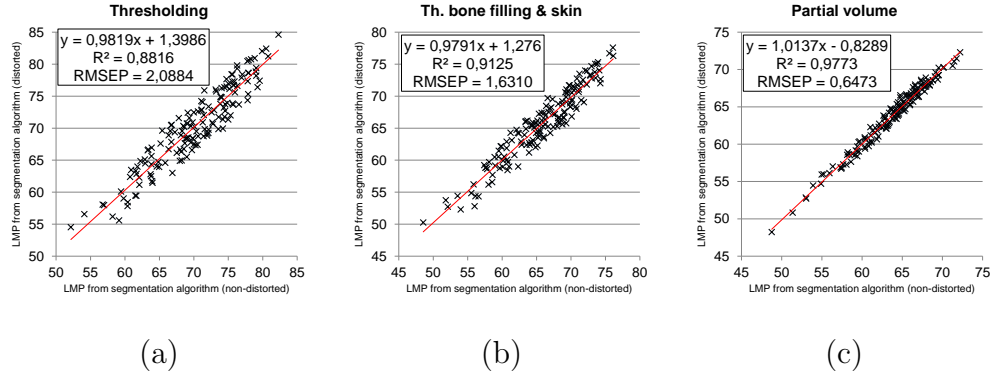


Figure 13: Correlation between the distorted results and the ones without distortion for each method.

Dissection methodology	Compared correlations	min	max	Steiger
Partial	PVD vs. ThD	< 0.0001	< 0.0001	< 0.0001
	PVD vs. ThBSD	0.0003	0.0022	0.0004
Total	PVD vs. ThD	< 0.0001	0.0055	< 0.0001
	PVD vs. ThBSD	0.0029	0.0237	0.0045
None (dist. vs. non-dist.)	PVD vs. ThD	< 0.0001	< 0.0001	< 0.0001
	PVD vs. ThBSD	< 0.0001	< 0.0001	< 0.0001

Table 5: P-values of the comparison between the methods' correlations with distortion for the partial and the total dissection methodologies, and also between the methods' correlations with or without distortion, showing the minimum and the maximum p-value from all the tests applied, and also the p-value of the Steiger's test (PVD = Partial volume with distortion, ThD = Thresholding with distortion, ThBSD = Thresholding with bone filling and skin detection with distortion).

396 To summarise, five main conclusions can be drawn from these five ex-  
397 periments. The first experiment has shown that the results from the whole

398 proposed approach outperform the results from the simple thresholding, and  
399 that they are as acceptable as the ones obtained from a part of the same  
400 pipeline, i.e. the thresholding method with bone filling and skin detection,  
401 so they can both be used indistinctly. From the second experiment, the need  
402 of estimating the tissues' density could not be demonstrated, so that only the  
403 volume has been taken into account. The convenience to detect the animal  
404 skin has been evaluated in the third experiment, which has determined that  
405 the accuracy of the LMP computation is higher when considering the skin  
406 as a new tissue. The fourth experiment has evaluated the results of applying  
407 the skin detection after the partial volume classification, but there has been  
408 no evidence of improvement, so that the order of the steps has remained the  
409 same. Finally, the fifth experiment has tested the different methods with  
410 distorted images, and the results prove that the proposed approach is much  
411 more robust to data variability than the other thresholding-based methods.

412 Note that correlation is higher, and RMSEP is lower, when total dissec-  
413 tion is considered instead of partial dissection. This is comprehensible since  
414 the carcasses were totally scanned, and this procedure is more similar to  
415 the total dissection than the partial dissection. In total dissection the lean  
416 of all the cuts of a carcass are separated manually and weighed; hence, the  
417 weight corresponds to the lean of the whole carcass (the same which has  
418 been scanned). In partial dissection, due to the reduction of the number of  
419 pieces to be dissected, the lean separated with a knife comes from the 4 main  
420 cuts and the tenderloin. Because of that, to obtain the LMP value of the  
421 whole carcass it is necessary to apply a scale factor, which was agreed to be  
422 the same for all EU countries (0.89) although there were some differences

423 between them. Thus, the use of this factor is a correction, and the LMP  
 424 value of the whole carcass is estimated from the lean of the 4 main cuts plus  
 425 the tenderloin. Furthermore, because of the way to compute the LMP values  
 426 from 4 cuts, the cutting has an important effect on the obtained lean, and  
 427 it is known that there are errors due to the cutting, especially in some cuts  
 428 (Nissen et al. (2006)), that may affect the accuracy of the LMP prediction.  
 429 The cutting errors are not so important in total dissection because all the  
 430 cuts are dissected and the total lean is obtained by knife. Probably, scan-  
 431 ning directly the main cuts would have given more precise results for partial  
 432 dissection, because the scanned cuts would have been the same used in the  
 433 prediction. In fact, Font-i-Furnols et al. (2009) showed a lower RMSEP for  
 434 the prediction of lean meat content of the carcasses obtained by partial dis-  
 435 section when the four main cuts were scanned (0.71%) than when the whole  
 436 carcass was scanned (0.82%).

#### 437 **4. Conclusion**

438 In this paper, a six-step pipeline (carcass detection, image thresholding,  
 439 bone filling, skin detection, partial volume classification and LMP computa-  
 440 tion), which includes a partial volume model and computes the LMP value  
 441 of a pig carcass, has been evaluated. The method is based on an already  
 442 presented pipeline, which has been extended by adding a new step to detect  
 443 the animal skin in the thresholding stage. The method has also been thor-  
 444 oughly tested with 146 half carcasses, and compared with a simple threshold-  
 445 ing method and a thresholding method with bone filling and skin detection,  
 446 which corresponds to an intermediate step of the proposed pipeline (from the

447 first to the fourth step). Five experiments have been designed to evaluate  
448 the accuracy and robustness of the method as well as the necessity of every  
449 step of the pipeline. The results of these experiments determine that the  
450 proposed approach is an accurate method to compute the LMP values of pig  
451 carcasses from CT scans, and that it is not as affected by data variability as  
452 the other evaluated methods are.

453 In the future, we intend to improve the bone tissue model from the ex-  
454 tended method, and apply the proposed approach to live pig CT scans. As  
455 for the latter, some efforts have been made to remove the internal organs  
456 which are present in the live pig CT images, but not required for the LMP  
457 computation (Xiberta et al. (2017)). Finally, the same automatic pipeline  
458 may be used to compute the LMP values of other species which may be of  
459 interest to the breeding companies and the meat industry.

## 460 **Acknowledgement**

461 This work has been funded in part by grants from the Spanish Govern-  
462 ment (Nr. TIN2016-75866-C3-3-R) and from the Catalan Government (Nr.  
463 2017-SGR-1101), and has been carried out as part of the BR-UdG grant  
464 (research fellowship from the Universitat de Girona). CERCA Programme  
465 (Generalitat de Catalunya) is also acknowledged.

## 466 **References**

467 Anton Bardera, Rubén Martínez, Imma Boada, Maria Font-i-Furnols, and  
468 Marina Gispert. VisualPork: towards the simulation of a virtual butcher.  
469 In *FAIM I: First Annual Conference on Body and Carcass Evaluation*,

470 *Meat Quality, Software and Traceability*, pages 97–98, 2012. Held in Tea-  
471 gasc Food Research Centre, Ashtown, Dublin, Ireland, 24th - 26th Septem-  
472 ber 2012.

473 Anton Bardera, Imma Boada, Albert Brun, Maria Font-i-Furnols, and Ma-  
474 rina Gispert. Quantification of computed tomography pork carcass images.  
475 In *2014 IEEE International Conference on Image Processing (ICIP)*, pages  
476 1688–1692, 2014. doi: 10.1109/ICIP.2014.7025338.

477 Maren Bernau, Prisca Valerie Kremer, Elisabeth Lauterbach, Ernst Tholen,  
478 Brigitte Kirkegaard Petersen, Elke Pappenberger, and Armin Man-  
479 fred Scholz. Evaluation of carcass composition of intact boars us-  
480 ing linear measurements from performance testing, dissection, dual en-  
481 ergy X-ray absorptiometry (DXA) and magnetic resonance imaging  
482 (MRI). *Meat Science*, 104:58–66, June 2015. ISSN 0309-1740. doi:  
483 10.1016/j.meatsci.2015.01.011.

484 Gonca Bural, Drew Torigian, Sandip Basu, Mohamed Houseni, Ying Zhuge,  
485 Domenico Rubello, Jayaram Udupa, and Abass Alavi. Partial volume  
486 correction and image segmentation for accurate measurement of standard-  
487 ized uptake value of grey matter in the brain. *Nuclear Medicine Com-*  
488 *munications*, 36(12):1249–1252, December 2015. ISSN 0143-3636. doi:  
489 10.1097/MNM.0000000000000394.

490 Anna Carabús, Marina Gispert, Albert Brun, Pedro López Rodríguez, and  
491 Maria Font-i-Furnols. In vivo computed tomography evaluation of the com-  
492 position of the carcass and main cuts of growing pigs of three commercial



crossbreeds. *Livestock Science*, 170:181–192, 2014. ISSN 1871-1413. doi:  
10.1016/j.livsci.2014.10.005.

Hwan Soo Choi, David R. Haynor, and Yongmin Kim. Partial volume tissue  
classification of multichannel magnetic resonance images - a mixel model.  
*IEEE Transactions on Medical Imaging*, 10(3):395–407, September 1991.  
ISSN 0278-0062. doi: 10.1109/42.97590.

Emre Şener, Erkan U. Mumcuoglu, and Salih Hamcan. Bayesian segmenta-  
tion of human facial tissue using 3D MR-CT information fusion, resolution  
enhancement and partial volume modelling. *Computer Methods and Pro-  
grams in Biomedicine*, 124:31–44, February 2016. ISSN 0169-2607. doi:  
10.1016/j.cmpb.2015.10.009.

Matthijs C. F. Cysouw, Gerbrand M. Kramer, Linda J. Schoonmade, Ronald  
Boellaard, Henrica C. W. de Vet, and Otto S. Hoekstra. Impact of  
partial-volume correction in oncological PET studies: a systematic review  
and meta-analysis. *European Journal of Nuclear Medicine and Molecu-  
lar Imaging*, 44(12):2105–2116, November 2017. ISSN 1619-7089. doi:  
10.1007/s00259-017-3775-4.

Gérard Daumas and Mathieu Monziols. An accurate and simple computed  
tomography approach for measuring the lean meat percentage of pig cuts.  
In *Proceedings of the 57th International Congress of Meat Science and  
Technology (ICoMST)*, pages 97–98, 2011. Held in Ghent, Belgium, 7th -  
12th August 2011.

Birk Diedenhofen and Jochen Musch. cocor: a comprehensive solution for the

516 statistical comparison of correlations. *PLoS ONE*, 10(4):e0121945, April  
517 2015. doi: 10.1371/journal.pone.0121945.

518 Andreas Dobrowolski, Róbert Romvári, Paul Allen, Wolfgang Branscheid,  
519 and Péter Horn. X-ray computed tomography as possible reference for  
520 the pig carcass evaluation [Schlachtkörperwertbestimmung beim schwein  
521 röntgen- computertomographie als mögliche referenzmethode]. *Fleis-  
522 chwirtschaft*, 84(3):109–112, 2004.

523 Juergen Dukart and Alessandro Bertolino. When structure affects function -  
524 the need for partial volume effect correction in functional and resting state  
525 magnetic resonance imaging studies. *PLoS ONE*, 9(12):e114227, December  
526 2014. doi: 10.1371/journal.pone.0114227.

527 Maria Font-i-Furnols, Maria Fabiana Teran, and Marina Gispert. Estimation  
528 of lean meat content in pig carcasses using X-ray Computed Tomography  
529 and PLS regression. *Chemometrics and Intelligent Laboratory Systems*, 98  
530 (1):31–37, 2009. ISSN 0169-7439. doi: 10.1016/j.chemolab.2009.04.009.

531 Maria Font-i-Furnols, Anna Carabús, Candido Pomar, and Marina Gispert.  
532 Estimation of carcass composition and cut composition from computed  
533 tomography images of live growing pigs of different genotypes. *Animal*, 9  
534 (1):166–178, January 2015. doi: 10.1017/S1751731114002237.

535 L. E. Gangsei, J. Kongsro, E. V. Olsen, M. Røe, O. Alvseike, and S. Sæbø.  
536 Prediction precision for lean meat percentage in Norwegian pig carcasses  
537 using 'Hennessy grading probe 7': evaluation of methods emphasized at  
538 exploiting additional information from computed tomography. *Acta Agri-*

- 539 *culturae Scandinavica, Section A — Animal Science*, 66(1):17–24, May  
540 2016. ISSN 0906-4702. doi: 10.1080/09064702.2016.1174292.
- 541 Rafael C. Gonzalez and Richard E. Woods. *Digital Image Processing*.  
542 Prentice-Hall, Upper Saddle River (NJ), USA, 2 edition, 2002. ISBN 0-  
543 201-18075-8.
- 544 Megan Jacobsen, Cayla Wood, and Dianna Cody. SU-G-206-07: dual-energy  
545 CT inter- and intra-scanner variability within one make and model. *Med-  
546 ical Physics*, 43(6Part25):3641–3641, June 2016. ISSN 2473-4209. doi:  
547 10.1118/1.4956948.
- 548 I. Jansons, V. Strazdina, R. Anenkova, D. Pule, I. Skadule, and L. Melece.  
549 Development of new pig carcasses classification formulas and changes in  
550 the lean meat content in Latvian pig population. *Agronomy Research*, 14  
551 (S2):1306–1314, 2016. ISSN 1406-894X.
- 552 Michael Judas, Reinhardt Höreth, and Wolfgang Branscheid. Computed  
553 tomography as a method to analyse the tissue composition of pig carcasses.  
554 *Fleischwirtschaft international*, 1/2007:56–59, 2007. ISSN 0179-2415.
- 555 Jørgen Kongsro, Morten Røe, Are Halvor Aastveit, Knut Kvaal, and Bjørg  
556 Egelanddal. Virtual dissection of lamb carcasses using computer to-  
557 mography (CT) and its correlation to manual dissection. *Journal of  
558 Food Engineering*, 88(1):86–93, September 2008. ISSN 0260-8774. doi:  
559 10.1016/j.jfoodeng.2008.01.021.
- 560 P. V. Kremer, M. Förster, and A. M. Scholz. Use of magnetic resonance  
561 imaging to predict the body composition of pigs in vivo. *Animal: an*

- 562 *International Journal of Animal Bioscience*, 7(6):879–884, 2013. doi:  
563 10.1017/S1751731112002340.
- 564 David H. Laidlaw, Kurt W. Fleischer, and Alan H. Barr. Partial-volume  
565 Bayesian classification of material mixtures in MR volume data using voxel  
566 histograms. *IEEE Transactions on Medical Imaging*, 17(1):74–86, February  
567 1998. ISSN 0278-0062. doi: 10.1109/42.668696.
- 568 Ramit Lamba, John P. McGahan, Michael T. Corwin, Chin-Shang Li, Tien  
569 Tran, J. Anthony Seibert, and John M. Boone. CT Hounsfield num-  
570 bers of soft tissues on unenhanced abdominal CT scans: variability be-  
571 tween two different manufacturers’ MCDT scanners. *American Journal of*  
572 *Roentgenology*, 203(5):1013–1020, November 2014. ISSN 0361-803X. doi:  
573 10.2214/AJR.12.10037.
- 574 Sangdae Lee, Santosh Lohumi, Hyoun-Sub Lim, Takafumi Gotoh, Byoung-  
575 Kwan Cho, and Samooel Jung. Determination of intramuscular fat con-  
576 tent in beef using magnetic resonance imaging. *Journal of the Faculty*  
577 *of Agriculture, Kyushu University*, 60(1):157–162, February 2015. ISSN  
578 0023-6152.
- 579 Dariusz Lisiak, Kamil Duziński, Piotr Janiszewski, Karol Borzuta, and  
580 Damian Knecht. A new simple method for estimating the pork car-  
581 cass mass of primal cuts and lean meat content of the carcass. *Ani-*  
582 *mal Production Science*, 55(8):1044–1050, 2015. ISSN 1836-0939. doi:  
583 10.1071/AN13534.
- 584 Dennis Mackin, Xenia Fave, Lifei Zhang, David Fried, Jinzhong Yang, Brian

585 Taylor, Edgardo Rodriguez-Rivera, Cristina Dodge, Aaron Kyle Jones,  
586 and Laurence Court. Measuring computed tomography scanner variability  
587 of radiomics features. *Investigative Radiology*, 50(11):757–765, November  
588 2015. ISSN 0020-9996. doi: 10.1097/RLI.0000000000000180.

589 Pia Marlene Nissen, Hans Busk, Marjatta Oksama, Marc Seynaeve, Marina  
590 Gispert, Pieter Walstra, Ingemar Hansson, and Eli Vibeke Olsen. The  
591 estimated accuracy of the EU reference dissection method for pig carcass  
592 classification. *Meat Science*, 73(1):22–28, May 2006. ISSN 0309-1740. doi:  
593 10.1016/j.meatsci.2005.10.009.

594 Lucien Nocera and James C. Gee. Robust partial-volume tissue classification  
595 of cerebral MRI scans. In *Proceedings of SPIE 3034, Medical Imaging 1997:*  
596 *Image Processing*, 1997. doi: 10.1117/12.274118. Held in Newport Beach,  
597 CA, United States, 22nd - 28th February 1997.

598 Eli Vibeke Olsen, Lars Bager Christensen, and Dennis Brandborg Nielsen.  
599 A review of computed tomography and manual dissection for cali-  
600 bration of devices for pig carcass classification - evaluation of uncer-  
601 tainty. *Meat Science*, 123:35–44, January 2017. ISSN 0309-1740. doi:  
602 10.1016/j.meatsci.2016.08.013.

603 Dzung L. Pham and Jerry L. Prince. Unsupervised partial volume esti-  
604 mation in single-channel image data. In *Proceedings IEEE Workshop on*  
605 *Mathematical Methods in Biomedical Image Analysis. MMBIA-2000*, pages  
606 170–177, 2000. doi: 10.1109/MMBIA.2000.852375. Held in Hilton Head  
607 Island, South Carolina, USA, 11th - 12th June 2000.

608 Róbert Romvári, Andreas Dobrowolski, Imre Repa, Paul Allen, Eli Vibeke  
609 Olsen, András Szabó, and Péter Horn. Development of a computed to-  
610 mographic calibration method for the determination of lean meat content  
611 in pig carcasses. *Acta Veterinaria Hungarica*, 54(1):1–10, January 2006.  
612 ISSN 0236-6290. doi: 10.1556/AVet.54.2006.1.1.

613 Su Ruan, Cyril Jaggi, Jinghao Xue, Jalal Fadili, and Daniel Bloyet. Brain tis-  
614 sue classification of magnetic resonance images using partial volume model-  
615 ing. *IEEE Transactions on Medical Imaging*, 19(12):1179–1187, December  
616 2000. ISSN 0278-0062. doi: 10.1109/42.897810.

617 Lauren E. Salminen, Thomas E. Conturo, Jacob D. Bolzenius, Ryan P.  
618 Cabeen, Erbil Akbudak, and Robert H. Paul. Reducing CSF partial vol-  
619 ume effects to enhance diffusion tensor imaging metrics of brain microstruc-  
620 ture. *Technology & Innovation*, 18(1):5–20, May 2016. ISSN 1949-8241.  
621 doi: 10.21300/18.1.2016.5.

622 Peter Santago and Howard Donald Gage. Quantification of MR brain images  
623 by mixture density and partial volume modeling. *IEEE Transactions on*  
624 *Medical Imaging*, 12(3):566–574, September 1993. ISSN 0278-0062. doi:  
625 10.1109/42.241885.

626 James H. Steiger. Tests for comparing elements of a correlation matrix.  
627 *Psychological Bulletin*, 87(2):245–251, March 1980. ISSN 0033-2909. doi:  
628 10.1037/0033-2909.87.2.245.

629 Rolf Symons, Justin Z. Morris, Colin O. Wu, Amir Pourmorteza, Mark A.  
630 Ahlman, João A. C. Lima, Marcus Y. Chen, Marissa Mallek, Veit Sandfort,

631 and David A. Bluemke. Coronary CT angiography: variability of CT scan-  
632 ners and readers in measurement of plaque volume. *Radiology*, 281(3):737–  
633 748, December 2016. ISSN 0033-8419. doi: 10.1148/radiol.2016161670.

634 The Commission of the European Communities. Commission Regulation  
635 (EC) No 1249/2008 of 10 December 2008 laying down detailed rules on  
636 the implementation of the Community scales for the classification of beef,  
637 pig and sheep carcass and the reporting of prices thereof. *Official Journal*  
638 *of the European Union*, L 337:3–30, December 2008.

639 The European Commission. Commission Delegated Regulation (EU)  
640 2017/1182 of 20 April 2017 supplementing Regulation (EU) No 1308/2013  
641 of the European Parliament and of the Council as regards the Union scales  
642 for the classification of beef, pig and sheep carcasses and as regards the re-  
643 porting of market prices of certain categories of carcasses and live animals.  
644 *Official Journal of the European Union*, L 171:74–99, April 2017.

645 Jussi Tohka. Partial volume effect modeling for segmentation and tissue  
646 classification of brain magnetic resonance images: a review. *World Jour-*  
647 *nal of Radiology*, 6(11):855–864, November 2014. ISSN 1949-8470. doi:  
648 10.4329/wjr.v6.i11.855.

649 Koen Van Leemput, Frederik Maes, Dirk Vandermeulen, and Paul Suetens.  
650 A unifying framework for partial volume segmentation of brain MR im-  
651 ages. *IEEE Transactions on Medical Imaging*, 22(1):105–119, January  
652 2003. ISSN 0278-0062. doi: 10.1109/TMI.2002.806587.

653 Martin Vester-Christensen, Søren G. H. Erbou, Mads F. Hansen, Eli V.

- 654 Olsen, Lars B. Christensen, Marchen Hviid, Bjarne K. Ersbøll, and Rasmus  
655 Larsen. Virtual dissection of pig carcasses. *Meat Science*, 81(4):699–704,  
656 2009. ISSN 0309-1740. doi: 10.1016/j.meatsci.2008.11.015.
- 657 Pieter Walstra and Gerard S. M. Merkus. Procedure for assessment of the  
658 lean meat percentage as a consequence of the new EU reference dissection  
659 method in pig carcass classification: based on discussion in the EU Man-  
660 agement Committee on Pig Meat and based on discussions with dissection  
661 experts during a meeting on 18-19, 1994 at Zeist, NL. Technical Report  
662 ID-DLO 96.014, DLO Institute for Animal Science and Health, Lelystad,  
663 Netherlands, March 1996.
- 664 Pau Xiberta, Imma Boada, Anton Bardera, and Maria Font-i-Furnols. A  
665 semi-automatic and an automatic segmentation algorithm to remove the  
666 internal organs from live pig CT images. *Computers and Electron-*  
667 *ics in Agriculture*, 140:290–302, August 2017. ISSN 0168-1699. doi:  
668 10.1016/j.compag.2017.06.003.